Int. J. Heat Mass Transfer. Vol. 25, No. 2, pp. 267–275, 1982
Printed in Great Britain

0017–9310/82/020267–09 $03.00/0

HEAT TRANSFER DURING THE SHOCK-INDUCED IGNITION OF AN EXPLOSIVE GAS

H. HEPERKAN and R. GREIF

University of California, Berkeley, Lawrence Berkeley Laboratory,
Energy and Environment Division

and

Department of Mechanical Engineering, Berkeley, CA 94720, U.S.A.

(*Received* 24 *February* 1981 *and in revised form* 31 *July* 1981)

Abstract—An experimental and theoretical study has been made of the unsteady heat transfer during the shock-induced ignition of an explosive gas. The heat flux at the end wall is obtained from measurements that were made with a thin film resistance thermometer. A separate analysis is based on the solution of the boundary layer equations in the gas near the end wall. Comparison of these results yields the instantaneous position of the reaction zone and the temperature distribution in the gas.

NOMENCLATURE

a, exponent in thermal conductivity relation;
c, specific heat;
c_p, specific heat at constant pressure;
h, heat transfer coefficient;
k, thermal conductivity;
K, dimensionless thermal conductivity;
p, pressure;
q, heat flux;
t, time;
T, temperature;
u, velocity;
V, dimensionless variable;
x, distance.

Greek symbols

α, thermal diffusivity;
γ, ratio of specific heats;
δ, thickness of gas layer;
η, similarity variable;
θ, dimensionless temperature;
ρ, density;
τ, transformed time variable;
ψ, transformed space variable;
ψ_{BF}, location of combustion zone.

Subscripts

c, combustion zone;
g, gas;
i, initial;
I, ignition;
s, solid;
w, wall;
∞, edge of gas boundary layer.

INTRODUCTION

THIS PAPER reports on an experimental and analytical study of the unsteady heat transfer occurring prior to and during a combustion reaction. The study is made in a shock tube in the region behind the reflected shock wave. Previous shock tube research has emphasized the dynamic effects resulting from the exothermic processes that occur in the course of a combustion reaction (e.g. Oppenheim *et al.* [1]). The present work utilizes these results as well as the experimentally determined wall heat flux reported herein to model the transport phenomena in the region near the wall. In particular, a thermal boundary layer is assumed which yields the instantaneous position of the reaction zone.

The study has been carried out with a mixture of hydrogen and oxygen with argon as the diluent. Reproducibility of the results was demonstrated and a separate study with pure argon was also made.

EXPERIMENTAL APPARATUS AND MEASUREMENTS

The measurements were made in an aluminum shock tube of rectangular cross-section, 38.4 mm ($1\frac{1}{2}''$) by 44.8 mm ($1\frac{3}{4}''$). Experiments were carried out with an inert gas, argon, and with a combustible mixture of $2H_2 + O_2 + 27A$ as the test or driven gases on the low pressure side of the diaphragm. The driver gas, on the high pressure side, was helium.

Two Kistler pressure transducers (S/N 52036) were mounted on the top of the test (or expansion) section to detect the arrival of the shock wave at their respective locations. The resulting signals were recorded on a Tektronix dual beam oscilloscope. The transducers were placed 101.6 mm (4.00″) apart. The travel time of the shock wave between the pressure

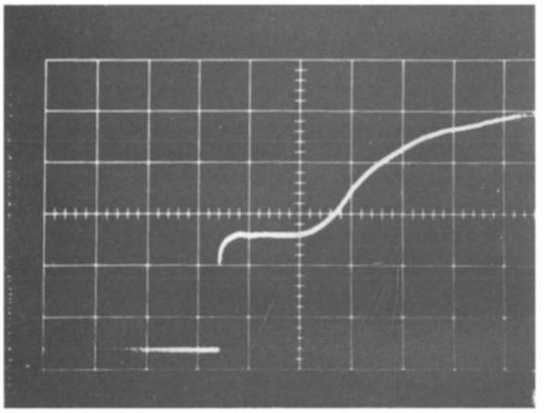

FIG. 1. Surface temperature measurement, reading gas. Time scale = 20 μs/cm; pre-ignition temp. increase = 4.6 K = 8.3 R; $2H_2 + O_2 + A$; run 214.

transducers was determined from measurements made with a Hewlett–Packard electronic digital counter. From these measurements the speed of the shock wave was determined. The sound speed was determined from the measurement of the initial temperature of the test gas. The resulting values of the Mach number, along with the initial temperature and pressure, permit the calculation of the temperature and the pressure behind the incident shock wave and behind the shock wave that reflects off the end wall.

To measure the temperature at the end wall as a function of time, a thin film resistance thermometer was used [2–12]. This gauge consisted of a thin platinum film that was painted and baked on a ceramic base, Macor, made by Corning Glass Works. The gauge was mounted flush with the wall. A temperature change caused a change in the resistance of the platinum film and the corresponding voltage was recorded (cf. Fig. 1). The resistance thermometer was calibrated in a thermally controlled enclosure so that the wall temperature variation could then be determined from the voltage output. The value of the resulting heat flux is dependent upon the parameter $(\rho c k)^{1/2}$ of the insulating ceramic base. This value is 1380 $Ws^{1/2}/m^2K$ (0.033 $Cal/cm^2CS^{1/2}$) for Macor [11, 12]. Many studies have been carried out with thin film resistance thermometers [2–12]. These studies have demonstrated the durability of these gauges and their rapid response times, which are of the order of one microsecond.

Measurements with the combustible mixture $[2H_2 + O_2 + 27A]$ were carried out for two nominally identical runs: 214 and 219, corresponding to initial pressures of 12.69 kPa (1.84 psia) and 12.72 kPa (1.85 psia); initial temperatures of 296.9 K (534.5 R) and 297.3 K (535.1 R); Mach numbers of 2.35 and 2.39. The values of the pressure and the temperature immediately after shock wave reflection are 30.96 kPa (44.9 psia) and 32.59 kPa (47.3 psia); 1317 K (2371 R) and 1337 K (2407 R).

ANALYSIS

The determination of the heat flux during shock wave heating is based on the measured surface temperature of a thermally infinite solid (Macor) that is initially at a constant temperature. The solution for the wall heat flux is given by [5]:

$$q_{ws} = \left(\frac{k\rho c}{\pi}\right)_s^{1/2} \int_0^t \frac{1}{(t-\bar{t})^{1/2}} \frac{dT_w}{d\bar{t}} d\bar{t}. \tag{1}$$

To perform the numerical calculations for the heat flux it is more convenient to use the following form of equation (1) [5]:

$$q_{ws} = \left(\frac{k\rho c}{\pi}\right)_s^{1/2} \left[\frac{T_w(t) - T_i}{t^{1/2}} + \frac{1}{2}\int_0^t \frac{T_w(t) - T_w(\bar{t})}{(t-\bar{t})^{3/2}} d\bar{t}\right] \tag{2}$$

which does not involve the evaluation of derivatives.

In the absence of combustion the end wall temperature rapidly increases to a value T_w that remains constant [5]. For this condition the wall heat flux is given by

$$q_{ws} = \left(\frac{k\rho c}{\pi}\right)_s^{1/2} \frac{T_w - T_i}{t^{1/2}}. \tag{3}$$

An alternative evaluation of the wall flux may be obtained from a solution of the conservation equations in the gas. The gas in the end wall region undergoes a rapid increase in temperature due to compression from both the incident and the reflected shock waves. The effect of the wall is to cool the gas in a boundary layer which grows with time. Neglecting viscous dissipation and species diffusion and taking the pressure to be uniform, because of the small velocities in the wall region, yields the following 1-dim. equations of continuity and energy [6–12]:

$$\frac{\partial \rho}{\partial t} + \frac{\partial}{\partial x}(\rho u) = 0, \tag{4}$$

$$\rho c_p \frac{\partial T}{\partial t} + \rho u c_p \frac{\partial T}{\partial x} = \frac{dp}{dt} + \frac{\partial}{\partial x}\left(k\frac{\partial T}{\partial x}\right), \tag{5}$$

where x is the coordinate perpendicular to the end wall. The continuity equation is satisfied by a stream coordinate ψ according to

$$\frac{\partial \psi}{\partial x} = \frac{\rho}{\rho_{ig}}, \quad \frac{\partial \psi}{\partial t} = -\frac{\rho u}{\rho_{ig}}, \tag{6}$$

where ρ_{ig} is the initial constant density of the gas after shock wave reflection. The energy equation in ψ, t coordinates is then given by

$$\rho c_p \frac{\partial T}{\partial t} = \frac{dp}{dt} + \frac{\rho}{\rho_{ig}} \frac{\partial}{\partial \psi}\left(k \frac{\rho}{\rho_{ig}} \frac{\partial T}{\partial \psi}\right). \tag{7}$$

During the pre-ignition period, corresponding to about the first 20 μs after the shock wave has reflected off the end wall, the pressure is constant and results for the heat transfer may be readily obtained. This interval is followed by ignition which takes place in a plane close to the end wall. This is accompanied by a

detonation wave which propagates away from the end wall and a diffusion transport which proceeds towards the wall. In view of the different phenomena occurring in the pre-ignition and combustion periods, it is convenient to consider them separately.

Pre-ignition period

During this interval the pressure is constant and the analysis is identical to that for an inert gas [6–9]. Briefly, the energy equation becomes:

$$\frac{1}{\alpha_{ig}}\frac{\partial\theta}{\partial t}=\frac{\partial}{\partial\psi}\left[\frac{K}{\theta}\frac{\partial\theta}{\partial\psi}\right], \tag{8}$$

where $\theta = T/T_{ig}$, $T_{ig} = T_\infty = T_5^*$, $K = k/k_{ig}$, $\alpha_{ig} = k_{ig}/\rho_{ig}\, c_p$.

Note that for an ideal gas at constant pressure $\rho/\rho_{ig} = T_{ig}/T = 1/\theta$. The initial and boundary conditions are:

$$T(\psi,0) = T_{ig}, \quad T(0,t) = T_w, \quad T(\infty,t) = T_{ig}. \tag{9}$$

The end wall location corresponds to $\psi = 0$.

Since there is no characteristic length or time in the problem, it is apparent that θ is a function only of $\psi^2/\alpha_{ig}t$ [6–9]. This requires that the wall surface temperature, T_w, be a constant which is in agreement with the experimental results [6–9]. Therefore we let $\eta = \psi/(2\alpha_{ig}t)^{1/2}$ and obtain

$$\frac{\mathrm{d}}{\mathrm{d}\eta}\left[\frac{K(\theta)}{\theta}\frac{\mathrm{d}\theta}{\mathrm{d}\eta}\right]+\eta\frac{\mathrm{d}\theta}{\mathrm{d}\eta}=0, \tag{10a}$$

$$\theta(0)=1, \quad \theta(\infty)=\frac{T_\infty}{T_w}=\frac{T_{ig}}{T_w}. \tag{10b}$$

Using a power law dependence for the thermal conductivity, $K = k/k_{ig} = (T/T_{ig})^a$, with a value for a, completes the specification of the problem [8, 9]. For $a = 1.0$ the heat flux obtained from equations (10a) and (10b) is given by

$$q_{wg} = k_{ig}\frac{(T_\infty - T_w)}{\sqrt{\pi\,\alpha_{ig}\,t}}. \tag{11}$$

This result is also given in the Appendix. For $a = 0.7$ [8, 9, 14] the heat flux q_{wg} is obtained from a numerical solution to equation (10a) subject to equation (10b) [8, 9].

Combustion period

The next interval includes the effects of combustion and now the pressure is time dependent. The energy equation in ψ, t coordinates is now given by

$$\frac{\partial T}{\partial t}=\frac{\gamma-1}{\gamma}\frac{T}{p}\frac{\mathrm{d}p}{\mathrm{d}t}+\alpha_{ig}\frac{p}{p_{ig}}T_{ig}^{1-a}\frac{\partial}{\partial\psi}\left(T^{a-1}\frac{\partial T}{\partial\psi}\right). \tag{12}$$

Introducing

$$V=\left(\frac{T}{T_{ig}}\right)^a\left(\frac{p}{p_{ig}}\right)^{a(1-\gamma)/\gamma} \quad \text{and} \quad \mathrm{d}\tau=\left(\frac{p}{p_{ig}}\right)^{(a\gamma-a+1)/\gamma}\mathrm{d}t \tag{13}$$

yields

$$\frac{\partial V}{\partial\tau}=\alpha_{ig}V^{(a-1)/a}\frac{\partial^2 V}{\partial\psi^2}. \tag{14}$$

The initial and boundary conditions are:

$$V(\psi,\tau_1) = fcn(\psi), \tag{15a}$$

$$V(0,\tau)=\left(\frac{T_w}{T_{ig}}\right)^a\left(\frac{p}{p_{ig}}\right)^{a(1-\gamma)/\gamma}, \tag{15b}$$

$$V(\delta,\tau)=\left(\frac{T_c}{T_{ig}}\right)^a\left(\frac{p}{p_{ig}}\right)^{a(1-\gamma)/\gamma}. \tag{15c}$$

The transformed time τ_1 is defined to be the time at the beginning of the combustion period which is the same as the time at the end of the pre-ignition period. Equation (15a) is the calculated distribution at the end of the pre-ignition period which is obtained from the solution of equations (10a) and (10b). The temperature of the combustion zone, T_c, along with the location of the combustion zone, δ, are required and these are discussed in the next section. For completeness it is noted that equation (14) was solved numerically using an explicit finite difference method to calculate the temperature profiles and the heat flux q_{wg}. A time increment, $\Delta\tau$, or 1 μs and a space increment, $\Delta\psi$, of 15 μm were used to satisfy the stability criteria for the numerical calculations [19].

RESULTS AND DISCUSSION

It is important to emphasize that the determination of the wall heat flux, q_{ws}, only requires the specification of the thermal properties of the ceramic solid and the temperature difference, $T_w - T_i$, in the solid. During the pre-ignition period the wall temperature is constant and the heat flux, q_{ws}, is then obtained from the simple relation, equation (3).

The determination of the heat flux, q_{wg}, during the pre-ignition period was previously presented [cf. equations (8–11)]. Briefly, during this period the pressure, p, the wall temperature, T_w, and the temperature outside the boundary layer, T_∞, are constant and the phenomena and analysis are identical to that for the inert gas problem [6–9]. The heat transfer, q_{wg}, is determined from the solution of the energy equation, equation (10a), subject to the conditions of equation (10b). A comparison of the values obtained for the heat

* T_{ig} is the temperature of the gas immediately after the shock wave has reflected off the end wall (Liepmann and Roshko [13]). The subscript ig is used to distinguish this from the initial (room temperature) condition in the solid as used in equations (2) and (3).

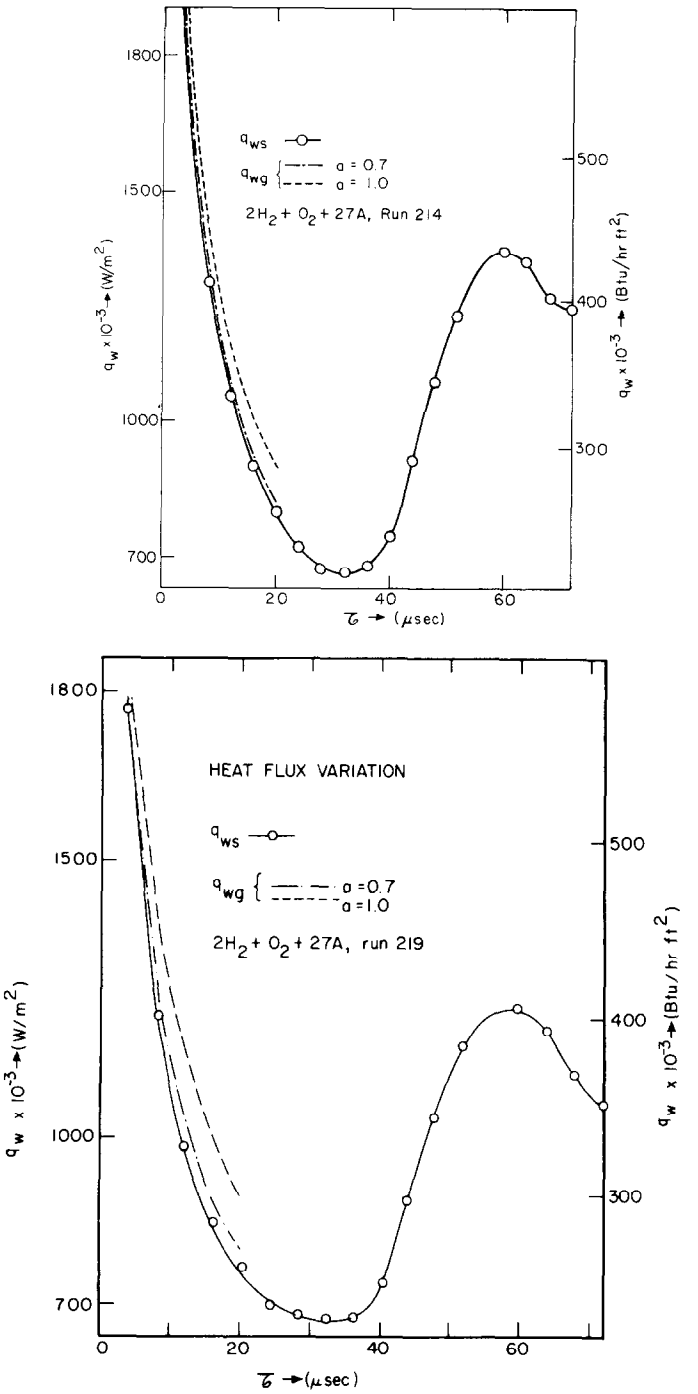

FIGS. 2(a) and (b). Heat flux variation.

fluxes, q_{wg}, with $a = 0.7$ and $a = 1.0$* [8, 9, 14] and, q_{ws}, as obtained from equation (3) is presented in Figs. 2(a) and (b). During the pre-ignition period, which corresponds to the first 20 μs after shock wave reflection, the heat fluxes agree to within 4 and 6% for Figs. 2(a) and (b), respectively. For runs with pure argon the agreement was 8% and 3% for two runs.

Recall that during the pre-ignition period the pressure is constant so that $\tau = t$. The heat flux decreases during this interval because the temperature difference across the thermal boundary layer in the gas, $T_\infty - T_w$, is constant while the thickness of the layer is increasing with time. The heat fluxes in Figs. 2(a) and (b) show this decrease during the pre-ignition period.

When combustion begins, the temperature of the gas in the reaction zone rapidly increases and this effect diffuses to the end wall where it increases the wall

* The result for $a = 1.0$ is discussed in the Appendix.

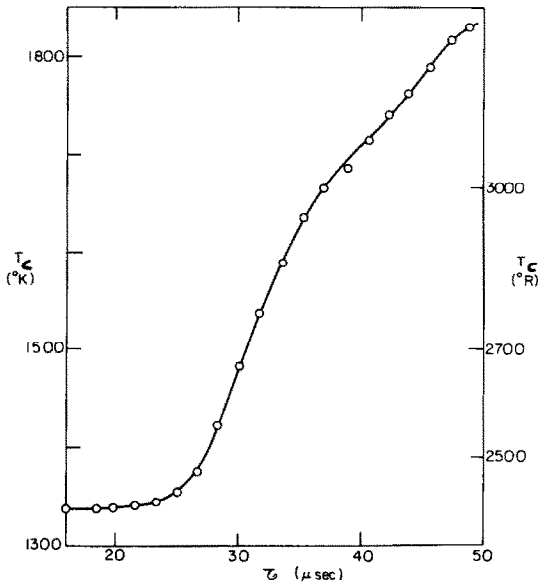

FIG. 3. Temperature variation for the reacting zone.

temperature (cf. Fig. 1) and increases (or retards the rate of decrease of) the wall flux. This variation of the heat flux, q_{ws}, is shown in Figs. 2(a) and (b).

The determination of the heat flux, q_{wg}, requires information relevant to the gas transport. From the work of Oppenheim *et al.* [1], Cohen *et al.* [15–17], and Cheng [18] the induction or 'ignition' time* is 20 μs after the shock wave has reflected off the end wall. The reaction is initiated at this time and is assumed to take place at the penetration depth or boundary layer thickness, δ; i.e. the location where the temperature reaches 99% of the free stream value. From the analysis during the pre-ignition period the penetration depth

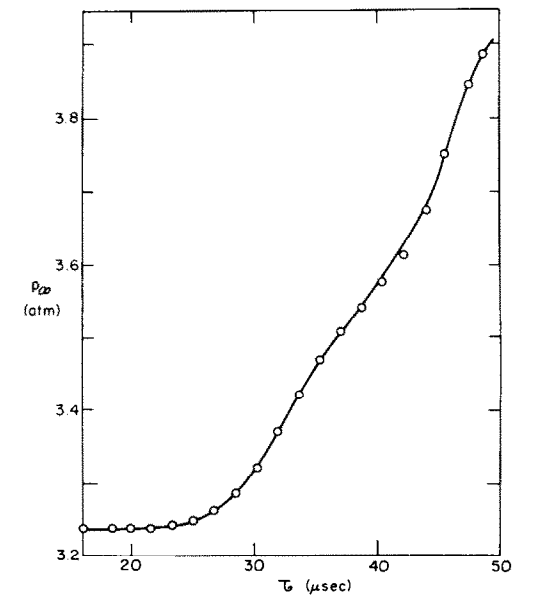

FIG. 4. Pressure variation in the gas layer.

*This is designated as the pre-ignition period.

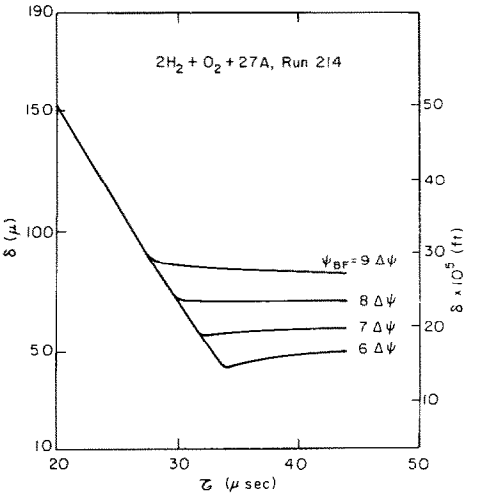

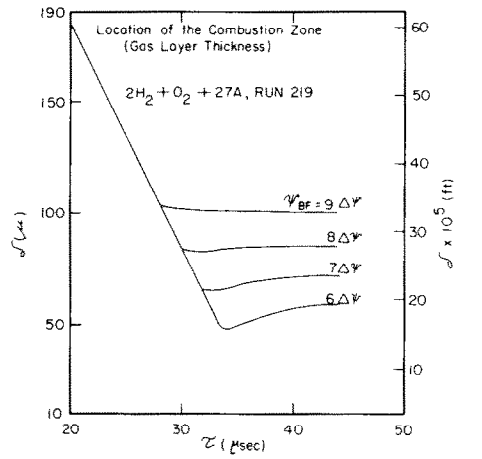

FIGS. 5(a) and (b). Location of the combustion zone.

and the temperature distribution are determined as a function of time and at $\tau = \tau_I = 20\,\mu$s this gives the initial condition for the combustion period required in equation (15a). The calculations of the pressure, p, and the temperature of the reaction zone, T_c, during the course of the reaction were based on previous experiments and theoretical studies which included the gas dynamic phenomena and the chemical kinetics of the reaction [1, 15–18]. The values are shown in Figs. 3 and 4 for Run 214 and the values of τ are given in Table 1. The remaining consideration is the propagation of the reaction zone, $\delta(t)$. Once this quantity is obtained the energy transfer may be determined in accordance with the solution of equations (14) subject to equations (15). Note that the model is one of thermal transport with the effect of combustion to increase the temperature of the reaction zone.

Calculations were made for different trajectories for the reaction zone, $\delta(t)$, as shown in Figs. 5(a) and (b) and the corresponding values that were calculated for q_{wg} are shown in Fig. 6 for Run 214. The diffusion from the reaction zone to the wall proceeds in the same

Table 1. Values of the transformed time

$\tau(\mu s)$	Run 219 $t(\mu s)$	Run 214 $t(\mu s)$
0	0	0
10	10.0	10.0
20	20.0	20.0
21	21.0	21.0
22	22.0	22.0
23	23.0	23.0
24	24.0	24.0
25	25.0	25.0
26	26.0	26.0
27	27.0	27.0
28	28.0	28.0
29	29.0	29.0
30	29.9	29.9
31	30.9	30.9
32	31.9	31.9
33	32.8	32.8
34	33.8	33.8
35	34.7	34.7
36	35.7	35.7
37	36.6	36.6
38	37.5	37.5
39	38.5	38.5
40	39.4	39.4
41	40.3	40.3
42	41.2	41.2
43	42.1	42.1
44	43.0	43.0
45	43.9	43.9

manner for all the cases considered; the difference is solely that the propagation is stopped at a final or quenching distance at $\psi_{BF} = 9\Delta\psi$, $8\Delta\psi$, $7\Delta\psi$ or $6\Delta\psi$ ($\Delta\psi = 15.1\ \mu$m) for the various cases considered. The calculations were carried out with the temperature, T_c, at the same location for two consecutive time increments. In detail, for Run 214, values of T_c equal to 1338 K and 1339 K were applied at 196 μm for two

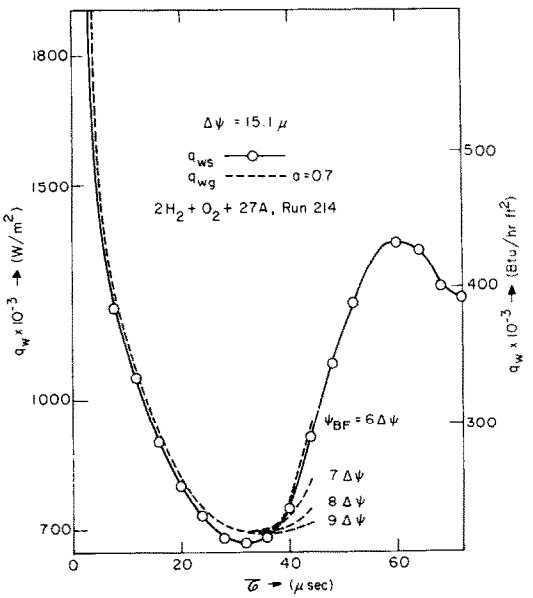

FIG. 6. Heat flux variations.

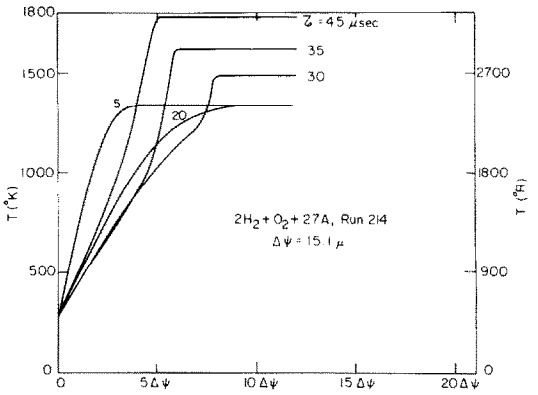

FIG. 7. Temperature distribution in the gas.

consecutive time steps; $T_c = 1342$ K and 1343 K were applied at 181 μm for the next two consecutive time steps etc. From the comparison of the fluxes, q_{ws} and q_{wg}, it is seen that the best agreement is achieved for the case $\psi_{BF} = 6\Delta\psi$ and the corresponding temperature distribution in the gas is shown at different times in Fig. 7.* Carrying out the transformation from ψ to x yielded the results shown in Figs. 5(a) and (b). For the case $\psi_{BF} = 6\Delta\psi$, the minimum value for δ for Run 214 is 44 μm which increases slightly to 50 μm at 45 μs (cf. Fig. 5a). This procedure was also carried out for the nominally identical Run 219 which was cited in the section on Experimental Apparatus and Measurements. For this case the minimum value for δ is 48 μm which increases to 59 μm at 45 μs (cf. Fig. 5b). Calculations were carried out until $\tau = 46\ \mu$s. At this time the detonation wave overtakes the reflected shock wave and values for the state of the gas were not available.

For clarification the case $\psi_{BF} = 6\Delta\psi$ is presented separately in Fig. 8(a) for Run 214 and in Fig. 8(b) for Run 219. For completness, the thermal conductivity variation $k/k_{ig} = (T/T_{ig})^1$, i.e. $a = 1$, is also shown which was discussed in the Appendix.

Of particular interest is the result for the variation of the heat transfer coefficient, h, which is defined by

$$h = \frac{q_w}{T_c - T_w}. \tag{16}$$

The results for h are presented in Fig. 9 with h_s based on q_{ws} and h_g based on q_{wg}. The heat transfer coefficient decreases during the pre-ignition period corresponding to the increase in the thickness of the boundary layer and the constant value for the temperature difference, $T_\infty - T_w$. During the combustion period the heat transfer coefficient decreases slightly and then increases as the effects of combustion diffuse to the end wall. The results for Run 219 are very close to those for Run 214 and are not shown.

* For clarification a schematic diagram is also presented in Fig. 10.

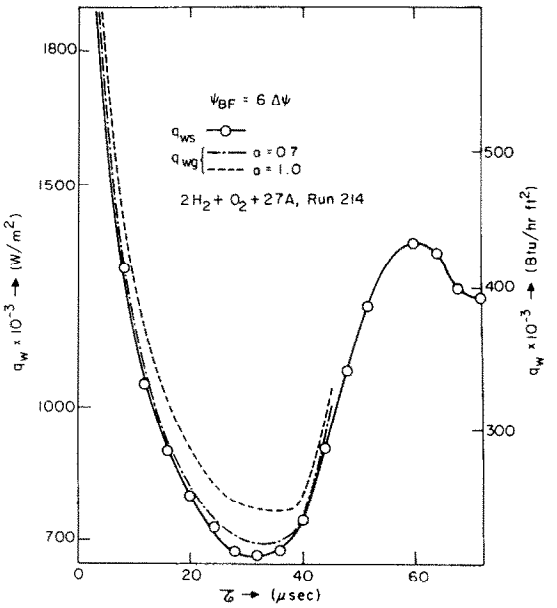

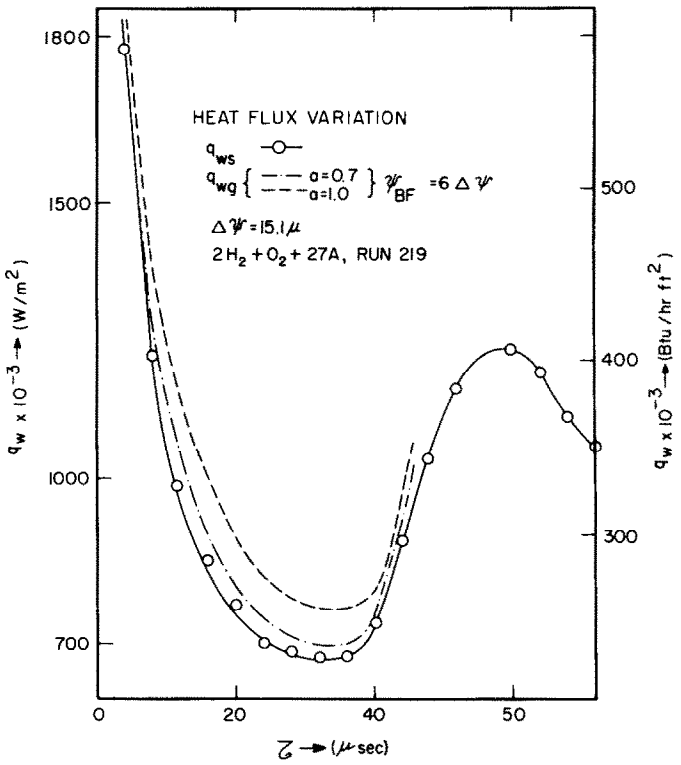

FIGS. 8(a) and (b). Heat flux variation.

In concluding, we note that it would have been desirable to carry out a study over a range of conditions, but this was not feasible because the related information that is required was not available. Indeed, the experimental and theoretical study of the gas dynamics and chemical kinetics of the hydrogen–oxygen system which were needed for the conditions studied in this work represented a substantial portion of the previous work that has been cited [1, 15–18]. The present work uses and extends these studies to include transport phenomena in the region near the wall. In particular, results have been presented for the first time for the wall heat flux and the location of the combustion zone as a function of time.

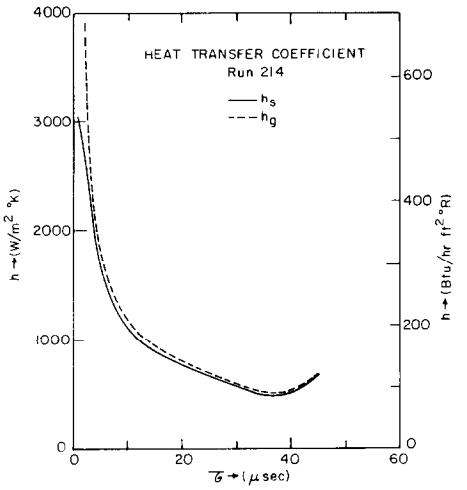

FIG. 9. Variation of the heat transfer coefficient.

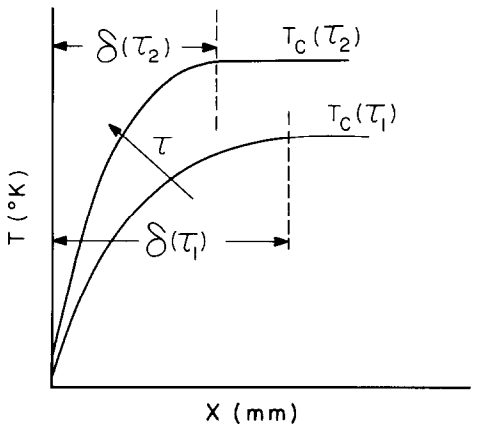

FIG. 10. Sketch of the temperature distribution in the gas.

Acknowledgement– It is a pleasure to acknowledge the interest and assistance of Professor A. K. Oppenheim, Dr. L. M. Cohen, K. Hom, A. Shaw and J. Naccache during the course of this research. The work was supported by the Office of Energy Research, Basic Energy Sciences, Division of the U.S. Department of Energy under Contract No. W-7405-ENG-48.

REFERENCES

1. A. K. Oppenheim, L. M. Cohen, J. M. Short, R. K. Cheng and K. Hom, Dynamics of the exothermic process in combustion, *15th Symposium (International) on Combustion, Tokyo*, pp. 1503–1513 (1974).
2. R. Vidal, Model instrumentation techniques for heat transfer and force measurements in a hypersonic shock tunnel. Report AD 917-A-1, Buffalo, N.Y., Cornell Aeronautical Laboratory, Inc. (1956).
3. J. Rabinowicz, M. E. Jessey and C. A. Bartsch, Resistance thermometer for heat transfer measurement in a shock tube. GALCIT Hypersonic Research Project Memo, 33, Guggenheim Aeronautical Laboratory, California Institute of Technology (July 1956).
4. P. H. Rose and W. I. Stark, Stagnation point heat transfer measurements in air at high temperature. Research Note 24, Everett, Mass., AVCO Research Laboratory, AVCO Manufacturing Corp. (December 1956).
5. J. G. Hall and A. Hertzberg, Recent advances in transient surface temperature thermomentry, *Jet Propulsion* **28,** 719–723 (1958).
6. M. Camac, J. A. Fay, R. M. Feinberg and N. H. Kemp, Heat transfer from high temperature argon, *Proc. 1963 Heat Transfer and Fluid Mechanics Institute*, p. 58. Stanford University Press, Calif. (1963).
7. M. R. Lauver, Shock tube thermal conductivity, *Phys. Fluids* **7,** 611 (1964).
8. D. J. Collins, R. Greif and A. E. Bryson, Measurements of the thermal conductivity of helium in the temperature range 1600-6700 K, *Int. J. Heat Mass Transfer* **8,** 1209–1216 (1965).
9. D. J. Collins, Shock tube study for the determination of the thermal conductivity of neon, argon and krypton, *ASME J. Heat Transfer* **88,** 52–56 (1966).
10. N. Isshiki and N. Nishiwaki, Study on laminar heat transfer of inside gas with cyclic pressure change on an inner wall of a cylinder head, *4th Int. Heat Transfer Conf., Paris–Versailles, 1970*, FC 3.5, pp. 1–10 (1970).
11. M. Nikanjam and R. Greif, Heat transfer during piston compression, *J. Heat Transfer* **100,** 527–530 (1978).
12. R. Greif, T. Namba and M. Nikanjam, Heat transfer during piston compression including side wall and convection effect, *Int. J. Heat Mass Transfer* **22,** 901–907 (1979).
13. H. W. Liepmann and A. Roshko, *Elements of Gas Dynamics*. John Wiley, New York (1957).
14. N. V. Tsederberg, *Thermal Conductivity of Gases and Liquids*. The M.I.T. Press, Cambridge (1965).
15. L. M. Cohen, Gasdynamic analysis of exothermic processes in combustion. Ph.D. dissertation, Dept. of Mech. Engng, Univ. of Calif., Berkeley, Calif. (1975).
16. L. M. Cohen, J. M. Short and A. K. Oppenheim, A computational technique for the evaluation of dynamic effects of exothermic reactions, *Combustion and Flame* **24,** 319–334 (1975).
17. L. M. Cohen and A. K. Oppenheim, Effects of size and dilution on dynamic properties of exothermic centers, *Combustion and Flame* **25,** 207–211 (1975).
18. R. Cheng, Induction Times and Strong Ignition Limits for mixtures of methane with hydrogen. Ph.D. dissertation, Dept. of Mech. Engng, Univ. of Calif., Berkeley, Calif. (1977).
19. H. A. Heperkan, Lawrence Berkeley Laboratory Report, LBL-10868 (May 1980).

APPENDIX

For a linear variation of the thermal conductivity with respect to temperature, $K = k/k_{ig} = (T/T_{ig})^a$, $a = 1.0$, equation (10a) becomes

$$\frac{d^2\theta}{\partial\eta^2} + \eta\frac{d\theta}{d\eta} = 0 \tag{A1}$$

subject to the conditions given in equation (10b). This linear problem may be readily solved and the result for the heat flux is

$$q_{ws} = k_{ig}\frac{(T_\infty - T_w)}{\sqrt{(\pi\alpha_{ig}t)}}. \tag{A2}$$

During the combustion period, the energy equation, equation (14), reduces to

$$\frac{\partial V}{\partial\tau} = \alpha_{ig}\frac{\partial^2 V}{\partial\psi^2} \tag{A3}$$

subject to the conditions

$$V(\psi,\tau_1) = fcn(\psi), \tag{A4a}$$

$$V(0,\tau) = \left(\frac{T_w}{T_{ig}}\right)\left(\frac{p}{P_{ig}}\right)^{(1-\gamma)/\gamma}. \quad \text{(A4b)}$$

$$V(\delta,\tau) = \left(\frac{T_c}{T_{ig}}\right)\left(\frac{p}{P_{ig}}\right)^{(1-\gamma)/\gamma}. \quad \text{(A4c)}$$

This problem has been solved numerically.

The case $a = 0.7$ corresponds to the correct thermal conductivity variation and the better agreement shown in Figs. 2(a) and (b) for $a = 0.7$ rather than 1.0 is in accord with this specification. The $a = 1.0$ case is appealing, however, because the resulting equations are simpler and the corresponding results, although not as accurate as those for the $a = 0.7$ case, are much more easily obtained and may be adequate for many applications.

TRANSFERT THERMIQUE PENDANT L'ALLUMAGE INDUIT PAR UN CHOC D'UN GAZ EXPLOSIF

Résumé—Une étude expérimentale et théorique concerne le transfert thermique non stationnaire pendant l'allumage induit par un choc d'un gaz explosif. Le flux thermique à la paroi est obtenu par des mesures faites à l'aide d'un thermomètre à résistance en film mince. Une analyse est basée sur la résolution des équations de couche limite dans la gaz près de la paroi. Une comparaison de ces résultats donne la position instantanée de la zone de réaction et la distribution de température dans le gaz.

WÄRMEÜBERTRAGUNG WÄHREND DER DURCH EINEN VERDICHTUNGSSTOSS AUSGELÖSTEN ZÜNDUNG EINES EXPLOSIVEN GASES

Zusammenfassung—Es wurde eine theoretische und experimentelle Studie zur instationären Wärmeübertragung während der durch einen Verdichtungsstoß ausgelösten Zündung eines explosiven Gases durchgeführt. Der Wärmestrom an der Stirnseite wird aus Messungen erhalten, die mit einem Dünnfilm-Widerstandsthermometer gemacht wurden. Eine getrennte Analyse stützt sich auf die Lösung der Grenzschichtgleichungen im Gas nahe der Stirnseite. Ein Vergleich dieser Resultate liefert die momentane Position der Reaktionszone und die Temperaturverteilung im Gas.

ТЕПЛОПЕРЕНОС ПРИ ИНДУЦИРОВАННОМ УДАРНОЙ ВОЛНОЙ ВОСПЛАМЕНЕНИИ ВЗРЫВЧАТОГО ГАЗА

Аннотация — Проведено экспериментальное и теоретическое исследование нестационарного процесса теплопереноса при воспламенении взрывчатого газа, индуцированном ударной волной. С использованием тонкопленочного термоанемометра сопротивления измерен тепловой поток на торец. Теоретический анализ основан на решении уравнений пограничного слоя для области газа у торцевой стенки. Сопоставление экспериментальных и теоретических результатов позволяет получить данные о положении зоны реакции в каждый момент времени и температурном распределении в газе.